The role of the cortical cytoskeleton: F-actin crosslinking proteins protect against osmotic stress, ensure cell size, cell shape and motility, and contribute to phagocytosis and development

Francisco Rivero[1],*, Bernd Köppel[1],*,[†], Barbara Peracino[2], Salvatore Bozzaro[2], Florian Siegert[3], Cornelis J. Weijer[3],[‡], Michael Schleicher[4], Richard Albrecht[1] and Angelika A. Noegel[1],[§]

[1]Max-Planck-Institut für Biochemie, Am Klopferspitz 18a, D-82152 Martinsried, Germany
[2]Dipartimento di Scienze Cliniche e Biologiche, Ospedale S. Luigi Gonzaga, Regione Gonzole 10, 10043 Orbassano-Torino, Italy
[3]Zoologisches Institut, Ludwig-Maximilians-Universität, Luisenstrasse 14, 80333 München, Germany
[4]Institut für Zellbiologie, Ludwig-Maximilians-Universität, Schillerstrasse 42, 80336 München, Germany

*These two authors have equally contributed to this work
[†]Present address: MRC Laboratory of Molecular Biology, Hills Road, Cambridge CB2 2QH, UK
[‡]Present address: Department of Anatomy and Physiology, Old Medical School, Dundee DD1 4AN, UK
[§]Author for correspondence

SUMMARY

We generated *Dictyostelium* double mutants lacking the two F-actin crosslinking proteins α-actinin and gelation factor by inactivating the corresponding genes via homologous recombination. Here we investigated the consequences of these deficiencies both at the single cell level and at the multicellular stage. We found that loss of both proteins severely affected growth of the mutant cells in shaking suspension, and led to a reduction of cell size from 12 μm in wild-type cells to 9 μm in mutant cells. Moreover the cells did not exhibit the typical polarized morphology of aggregating *Dictyostelium* cells but had a more rounded cell shape, and also exhibited an increased sensitivity towards osmotic shock and a reduced rate of phagocytosis. Development was heavily impaired and never resulted in the formation of fruiting bodies. Expression of developmentally regulated genes and the final developmental stages that were reached varied, however, with the substrata on which the cells were deposited. On phosphate buffered agar plates the cells were able to form tight aggregates and mounds and to express prespore and prestalk cell specific genes. Under these conditions the cells could perform chemotactic signalling and cell behavior was normal at the onset of multicellular development as revealed by time-lapse video microscopy. Double mutant cells were motile but speed was reduced by approximately 30% as compared to wild type. These changes were reversed by expressing the gelation factor in the mutant cells. We conclude that the actin assemblies that are formed and/or stabilized by both F-actin crosslinking proteins have a protective function during osmotic stress and are essential for proper cell shape and motility.

Key words: α-actinin, 120 kDa gelation factor, Development, Video microscopy, *Dictyostelium*

INTRODUCTION

The mechanical properties of the cytoplasm are important determiners of cell shape and cell motility and can therefore greatly influence morphogenesis and cell division. Actin filaments and proteins that crosslink the filaments and control their size are major contributors to the mechanical properties of the cytoplasm (Luby-Phelps, 1994). Cells contain a variety of actin filament crosslinkers that bind actin with a range of affinities, have different subcellular localizations, and are differently regulated. This combination allows cells to change the cytoplasm from a rigid to a dynamic network (Wachsstock et al., 1994). In *Dictyostelium discoideum* α-actinin and the 120 kDa gelation factor (ABP120) are major crosslinking proteins. They belong to a family of crosslinking proteins based on their homology in the actin-binding site and their similar overall

structure (Matsudaira, 1991). Both proteins are found throughout the cytoplasm, for the gelation factor an enrichment in pseudopods and an association with the Triton insoluble cytoskeleton during pseudopod formation have been reported (Condeelis et al., 1988). Using a rheological approach with a torsion pendulum it could be shown that the viscoelastic properties of F-actin gels crosslinked by either α-actinin or the 120 kDa gelation factor are different. α-actinin/F-actin networks responded to deformation with a strongly damped oscillation, whereas the gelation factor/F-actin networks reacted in a more elastic, weakly damped way (Janssen et al., 1996). This could explain on a functional basis the presence of many different F-actin crosslinking proteins at the same time and region in a cell. In addition, F-actin crosslinking proteins can serve as substitutes for large amounts of actin. It required only traces of *Dictyostelium* gelation factor in relatively weak filamentous

networks to reach the same viscoelastic strength as was found with high F-actin concentrations alone (Janssen et al., 1996). The individual input of different F-actin crosslinking proteins could be assayed even on whole *Dictyostelium* cells by using rheological methods, and it became obvious that lack of α-actinin caused a significant reduction of the viscoelastic response after deformation at high frequencies. These data suggest that in *Dictyostelium* amoebae α-actinin is responsible for organizing the cytoskeleton against fast and strong impacts from outside, whereas the 120 kDa gelation factor helps to build a three-dimensional meshwork of filaments as it is required in the cell cortex and during pseudopod formation (Eichinger et al., 1996).

One of the major advantages of the *Dictyostelium* system for studying these topics is the possibility to generate cytoskeletal mutants (Schleicher et al., 1995). For investigation of the 120 kDa gelation factor two mutants have been described, one was isolated after nitrosoguanidine-mutagenesis (Brink et al., 1990), in the second one the gene was inactivated using homologous recombination (Cox et al., 1992, 1996). The chemically induced mutant exhibited normal motile behavior, mutant cells isolated by gene disruption showed reduced pseudopod formation and a slower rate of translocation. Double mutants lacking α-actinin and gelation factor failed to complete the developmental cycle and the ability to form fruiting bodies was strongly reduced (Witke et al., 1992). The parent strains of these double mutants had been generated by chemical mutagenesis and were deficient in either α-actinin or gelation factor.

Since it is a concern that during nitrosoguanidine treatment of cells several genes might be affected, we have now used homologous recombination to specifically inactivate both genes by targeted disruption. Double and single mutants were analyzed at the single cell level and during multicellular development. Special emphasis was put on aspects that are controlled by the cortical actin cytoskeleton. In the double mutants we observed a cell size reduction, the generation of nucleus free particles, reduced resistance against osmotic shock, reduced rate of phagocytosis and altered cell shape and cell motility. A comparison with mutants lacking either α-actinin or 120 kDa gelation factor indicated that the proteins have a different impact on these properties and that they rather act in concert. Their combined loss leads to a general weakening of the cortical cytoskeleton with severe consequences for development.

MATERIALS AND METHODS

Dictyostelium strains and growth conditions

Dictyostelium discoideum strain AX2-214, an axenically growing derivative of wild strain NC-4, is the parent strain of all mutants. A gelation factor negative transformant (GHR) was generated by disrupting the gelation factor gene via homologous recombination. The transformation vector used was pDgel1.5 (Witke et al., 1992) carrying a 1.5 kb N-terminal *Eco*RI fragment of the gelation factor cDNA (Noegel et al., 1989). The isolation of mutants lacking α-actinin and gelation factor is described by Eichinger et al. (1996).

D. discoideum strain AX2 and mutant strains were either grown at 21°C in liquid nutrient medium with shaking at 160 rpm (Claviez et al., 1982) or on SM agar plates with *Klebsiella aerogenes* (Williams and Newell, 1976) or on nutrient agar plates with *Escherichia coli* B/2 (Noegel et al., 1985).

Construction of the gelation factor expression vector and isolation of mutants

To express the gelation factor in the G418- and phleomycin-resistant strain AGHR2, a vector was constructed which allowed expression under the control of the actin 15 promoter and actin 8 terminator (Knecht et al., 1986) using hygromycin as selection marker. The hygromycin-resistance gene from pDE109 (Egelhoff et al., 1989) was cloned into the *Sma*I and *Sal*I sites of pUC19 to generate pHY. This plasmid was linearized with *Hin*dIII, blunt-ended with S1-nuclease and ligated to a 0.8 kb fragment encoding the actin 15 promoter and actin 8 terminator derived from pDEX H (Faix et al., 1992). The resulting *Dictyostelium* expression vector pHEX contains a unique *Hin*dIII site between the actin 15 promoter and the actin 8 terminator which can be used for cloning. For expression of gelation factor, a 2.7 kb fragment encoding the full-length cDNA sequence was obtained from cDNA clone p1-10 (Noegel et al., 1989) using PCR and cloned into the *Hin*dIII site of pHEX to generate plasmid pHGE.

Transformation of *D. discoideum* was performed as described (Witke et al., 1987). For selection of hygromycin resistant transformants, cells were grown in HL-5 medium, pH 7.5 (Egelhoff et al., 1989). After transformation cells were allowed to recover overnight and selection was started with 3 μg/ml hygromycin B (Calbiochem, La Jolla, CA). Concentrations of the antibiotics were increased stepwise to 5, 7.5 and 10 μg/ml until control plates were cleared. Transformants were identified by colony blotting (Wallraff et al., 1986) using gelation factor specific monoclonal antibody 82-471-17 (Brink et al., 1990).

Western, Southern and northern blotting

SDS-polyacrylamide gel electrophoresis was done as described by Laemmli (1970). Western blotting was performed using ^{125}I-labelled antibodies or the ECL detection system (Amersham, Braunschweig, Germany). DNA and RNA were isolated as described (Noegel et al., 1985). After transfer to nylon membranes (Amersham), hybridization was performed at 37°C for 12-16 hours in hybridization buffer containing 50% formamide and 2× SSC. The blots were washed for 2× 5 minutes in 2× SSC containing 0.1% SDS at room temperature and 1× 60 minutes in wash buffer containing 50% formamide and 2× SSC at 37°C. ^{32}P-labelled probes were generated using a random prime labelling kit (Stratagene, La Jolla, CA).

Development of *Dictyostelium*

For analysis of development cells were allowed to develop on nitrocellulose filters (Millipore type HA, Millipore, Molsheim, France) at 21°C as described (Newell et al., 1969) or on phosphate-buffered agar plates (17 mM Soerensen phosphate buffer, pH 6.0). For development in shaking suspension cells were washed in Soerensen phosphate buffer, resuspended at a density of 1×10^7 cells/ml and shaken at 21°C and 150 rpm. Morphogenesis was studied by allowing cells to develop on 1.2% (w/v) water agar plates or phosphate-buffered agar plates. Development was also examined with cells growing on SM agar plates on a lawn of *K. aerogenes* (Williams and Newell, 1976) or on nutrient agar plates on a lawn of *E. coli* B/2 (Noegel et al., 1985).

Cell size determination

D. discoideum strain AX2 and mutant strains were grown in liquid medium until a density of 2×10^6 cells/ml was reached. Cells were washed with cold Soerensen phosphate buffer and left on ice for 20 minutes after vortexing. This procedure led to single essentially spherical cells. Cells were photographed and diameters determined from the prints. Furthermore, cell size distributions were also determined using a Coulter Counter ZM (Coulter Electronics, Luton, England).

Osmotic shock

Cells were grown to a density of 3×10^6 cells/ml, washed twice in Soerensen phosphate buffer and resuspended to a density of 3×10^7 cells/ml. The cells were kept shaking at 21°C and 160 rpm for 1 hour,

then sorbitol was added to a final concentration of 0.4 M and shaking was continued for 2 hours. At various time points samples were taken, diluted into Soerensen phosphate buffer containing *K. aerogenes* and plated onto SM agar plates to assay for viability. Cell lysis upon osmotic shock was also estimated by determining the protein content in the cellular pellet.

Phagocytosis microassay

Phagocytosis was measured by a modification of a previously described assay (Bozzaro et al., 1987). *E. coli* B/r at a final concentration of 1×10^{10}/ml were labelled with 0.1 mg/ml FITC (Sigma) as described by Vogel (1987), except that the incubation time and temperature were, respectively, 90 minutes and 23°C. *Dictyostelium* cells starved for 30 minutes in Soerensen phosphate buffer were mixed with cold FITC-labelled bacteria at a final concentration of 4×10^6 and 5×10^9/ml, respectively, in a final volume of 0.1 ml in 5 ml polystyrene tubes. The tubes were shaken at 200 vibrations per minute. At various time points the cells were washed free of unbound bacteria by diluting with 5 ml cold 50 mM Na-phosphate buffer, pH 9.2, and centrifuging at 110 *g* for 3 minutes. After an additional washing, the cell pellet was resuspended in 1 ml Na-phosphate buffer and lysed for 30 minutes with 0.2% Triton X-100. Fluorescence in cell lysates was measured in a spectrofluorimeter SFM 25 (Kontron) at an excitation wave length of 470 nm and emission wave length of 520 nm. To determine the number of bacteria, a calibration curve was made by serial dilutions of FITC-labeled bacteria lysed with 1% SDS for 2 minutes at 90°C (Vogel, 1987).

Chemotaxis

For qualitative evaluation of chemotaxis, cells were starved for 6 hours in Soerensen phosphate buffer in shaking suspension and transferred onto a glass surface. Cells were stimulated with a micropipette filled with 10^{-4} M cAMP and the ability of the cells to move towards the micropipette was examined (Gerisch and Keller, 1981; André et al., 1989). Quantitative analysis of cell motility and chemotaxis was performed using an image-processing system (Segall et al., 1987) and a chemotaxis chamber (Fisher et al., 1989) with a maximum cAMP concentration of 5×10^{-8} M (Brink et al., 1990).

Immunofluorescence studies

Cells were allowed to settle on a coverslip and fixed in cold methanol (−20°C). Profilin I and contact site A were detected with monoclonal antibodies 153-246-10 (Haugwitz et al., 1991) and 33-249-17 (Berthold et al., 1985), respectively, followed by incubation with Cy3 labelled anti-mouse IgG antibody according to the method of Weiner et al. (1993). Actin distribution was determined by incubation with an actin specific monoclonal antibody (Simpson et al., 1984). Nuclei were stained with 4′,6-diamidino-2-phenylindole (DAPI).

Synergy experiments

For synergy experiments AX2 cells expressing the green fluorescent protein under the control of the actin 15 promotor (AX2-gfp) (Rietdorf et al., 1996) or the bacterial β-galactosidase gene under the control of the actin 6 promoter (AX2-gal) (Dingermann et al., 1989) were mixed with AGHR2 cells at the vegetative stage and allowed to develop through aggregation to the mound stage. In some experiments AGHR2 cells labelled with rhodamine-dextran (Sigma), were mixed with 0.5% AX2-gfp cells before plating. For rhodamine-dextran labelling 1×10^7 AGHR2 cells were incubated with 1 ml rhodamine-dextran solution (10 mg/ml in KK2, 20 mM potassium phosphate buffer, pH 6.8). This cell suspension was then pressed once through a Nythal filter (Seidengazefabrik AG Thal, Switzerland) with 7 μm pore size. Thereby about 1-3% of the cells were labelled and retained the label for more than 24 hours (Siegert and Weijer, 1992). In the synergy experiments with AX2-gal cells the mounds were fixed and stained (Bichler and Weijer, 1994).

Videomicroscopy and digital image processing

Plates for videomicroscopy were prepared as previously described (Siegert and Weijer, 1989) and incubated at 21°C until mounds had formed. Video films of mounds were made by placing the agar plates on a Zeiss IM 35 inverted microscope equipped with ×6.3 or ×10 objectives and an image intensified CCD camera (SANYO VC 2512). Video images were captured at 5 or 10 second intervals and stored on a time-lapse video recorder (Sony EVT 801CE). In several experiments background noise was reduced by averaging 8-16 video images in real time (25 frames/second) before storing the result as a single image on the video recorder. Fluorescence measurements were conducted with a ×16 Neofluar objective and a high sensitvity SIT camera (Hamamatsu C2400-8). To reduce damage of the cells the excitation light was reduced 64 times by a grey filter and the camera was adjusted to maximum sensitivity. Between successive time points of the time lapse measurements (every 10 seconds) the excitation light was shut off by a computer controlled shutter.

Digital image processing was performed with an IBM compatible 486 66 Mhz computer equipped with an Imaging Technology board (AFG, resolution 768×512 pixel). Analysis of dark field waves was carried out essentially as previously described (Siegert and Weijer, 1989, 1995). Briefly, the gray values inside a narrow window placed across a mound were averaged along the short axis to create a one-dimensional representation of optical density values. These optical density slices were taken every 5 or 10 seconds and stored on a hard disc. For analysis successive measurements were placed below each other to obtain a time-space plot which was analyzed by other programs. The movement of single cells was measured by manually tracking fluorescent cells (Siegert and Weijer, 1992).

RESULTS

Disruption of the α-actinin and gelation factor genes

For disruption of the α-actinin and gelation factor genes we constructed vectors pΔAA and pΔGF which contain a marker gene between the 5′ and the 3′ coding sequences of the respective gene (Eichinger et al., 1996). AX2 cells were transformed with linearized plasmid pΔAA; G418 resistant transformants were cloned and tested with mAb 47-62-17 (Schleicher et al., 1988) to identify α-actinin negative cells. Restriction enzyme analysis showed that in eleven out of twelve independent α-actinin negative transformants a gene disruption had occurred, in one transformant (AHR) a gene replacement event was identified since an internal 0.7 kb *Eco*RI fragment of the gene was lacking. Mutant AHR cells were transformed with pΔGF for disruption of the gelation factor gene and transformants screened with mAb 82-471-14 (Brink et al., 1990). Two independent clones, AGHR1 and 2, lacking gelation factor were isolated. In both mutants inactivation of the gene was due to a gene disruption.

The gene replacement and disruption events were stably maintained, since after growth of AGHR1 and AGHR2 cells for more than 100 generations without selection pressure in liquid medium no revertants were observed when single colonies or whole cell extracts were analyzed by western blotting with specific antibodies.

In all subsequent analyses the following strains were assayed: strain AX2 as wild-type parent strain, strain AHR as α-actinin deficient transformant, strain GHR as gelation factor minus mutant in which the gene was disrupted by a single copy insertion of vector pDgel1.5 (Witke et al., 1992) and strains AGHR1 and 2 as double mutants (Fig. 1). Since both double
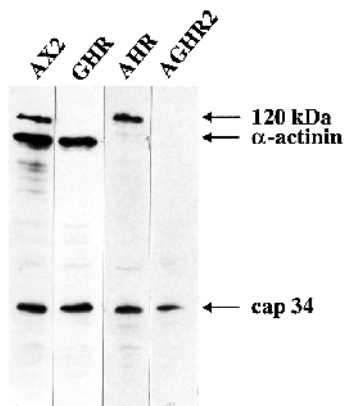
Fig. 1. Western blot analysis of wild-type and mutant strains. Total cellular protein from 2×10^5 cells of AX2 wild type, single mutants AHR and GHR and double mutant AGHR2 was separated by SDS-PAGE (10% acrylamide), blotted onto nitrocellulose and probed with α-actinin specific mAb 47-62-17 or gelation factor specific mAb 82-471-14. The blot was subsequently probed with cap34 specific mAb 409 (Hartmann et al., 1989) to show comparable loading.

mutant strains have similar characteristics, in most cases only the data for AGHR2 are shown.

Growth of the double mutant strains

When grown under axenic conditions AX2 wild-type cells as well as mutant cells of strains AHR and GHR reached final cell densities of 1×10^7 cells/ml and higher. In contrast, AGHR2 cells never reached similar densities and consistently stopped growth much earlier. The doubling time was also prolonged from 10 hours for AX2 to 19 hours for AGHR2 (Fig. 2). For AGHR2 cells we noted a substantial shedding of cellular material during growth in shaken suspension. These particles often had diameters of up to 3 μm. They contained cytosolic proteins as visualized by staining for profilin but were devoid of nuclei. This property could be traced back to a gelation factor deficiency since GHR cells exhibited a similar phenotype (Fig. 3).
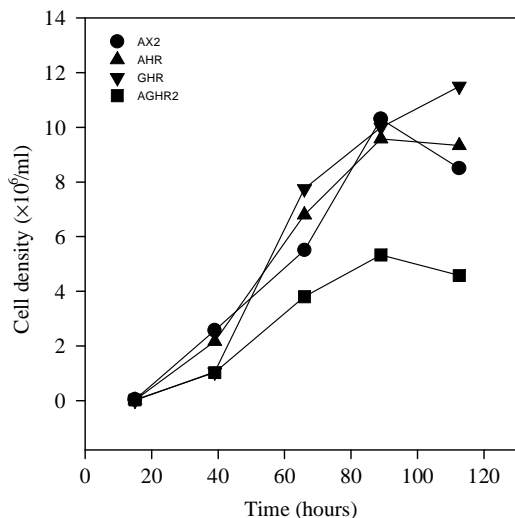

Fig. 2. Growth of wild-type and mutant cells in shaking culture. Growth of wild-type AX2, AHR and GHR in shaking suspension was comparable, whereas AGHR2 had a reduced growth rate and did not reach similar cell densities.

Cell size of AGHR mutants

AGHR2 cultures contained both smaller as well as significantly larger cells than wild-type cultures. For further analysis the size distribution of AGHR2 cells was determined and compared to the one of AX2, AHR and GHR cells (Fig. 4). Both AHR and GHR cells were almost indistinguishable in size from AX2 cells, with an average diameter of 12 μm whereas most AGHR2 cells had a diameter of 9 μm. In addition, there was a second population of enlarged AGHR2 cells with diameters of approximately 25 μm. This second population accounted for about 5% of the total cell number. Immunofluorescence studies using the DNA binding dye DAPI revealed that the large-sized AGHR2 cells were multinucleated. Determination of cell sizes in an automated counter supported the finding that the majority of AGHR2 cells was smaller than AX2 cells.

Response to osmotic shock

Exposure of cells to high osmolarities evokes a variety of responses. The accumulation of compatible osmolytes raises the internal osmotic potential and the synthesis of stress proteins protects cellular components facilitating repair and recovery (Kwon and Handler, 1995). Whereas these are slow processes that occur in pro- and eukaryotes, eukaryotic cells in addition can quickly respond to changes in cell volume by dis- and reassembly of their cytoskeletons. When wild-type and mutant cells were treated for up to two hours with 0.4 M sorbitol and then diluted into a solution of low osmolarity, survival of wild-type cells was much better than that of AGHR2 cells. The osmotic shock led to a marked reduction in the proportion of viable AGHR2 cells, which was 66% after one hour and 14% after two hours of treatment with sorbitol (Fig. 5). Comparable results were obtained when cell lysis was estimated by determining the decrease in protein content in the cellular pellet. No significant lysis was observed for AX2 cells and AHR and GHR were comparable to AX2 in their resistance to osmotic shock.

Phagocytosis of mutant strains

Immunofluorescence studies suggest that both crosslinkers are involved in different steps of the phagocytic process, gelation factor being located at the phagocytic cup (Cox et al., 1996) and α-actinin in phagosomes (Furukawa and Fechheimer, 1994). This has prompted us to test single and double mutants for their ability to phagocytose bacteria. After 30 minutes of incubation with fluorescently labelled *E. coli*, AGHR2 cells showed a significant reduction (40-60%) in the rate of bacterial uptake, compared to the single mutants and the wild-type strain AX2 (Fig. 6). As internal control we used HSB50, a severely impaired phagocytosis mutant, which is also defective in cell-substrate adhesion and is blocked at the mound stage of development (Ceccarelli and Bozzaro, 1992). In contrast to HSB50, the rate of phagocytosis in AGHR2 seems to be normal for the first 5 minutes, suggesting that the double mutation probably affects later steps in the phagocytic process more strongly.

Motility and chemotactic behavior of mutant strains

Chemotaxis of starving cells towards cAMP was analyzed in the capillary assay where cells are stimulated with a micropipette filled with cAMP (10^{-4} M). AGHR2 cells were able to move towards the pipette, however, they responded much more slowly than wild-type cells. In a typical experiment AX2 cells arrived at the pipette within a minute, whereas
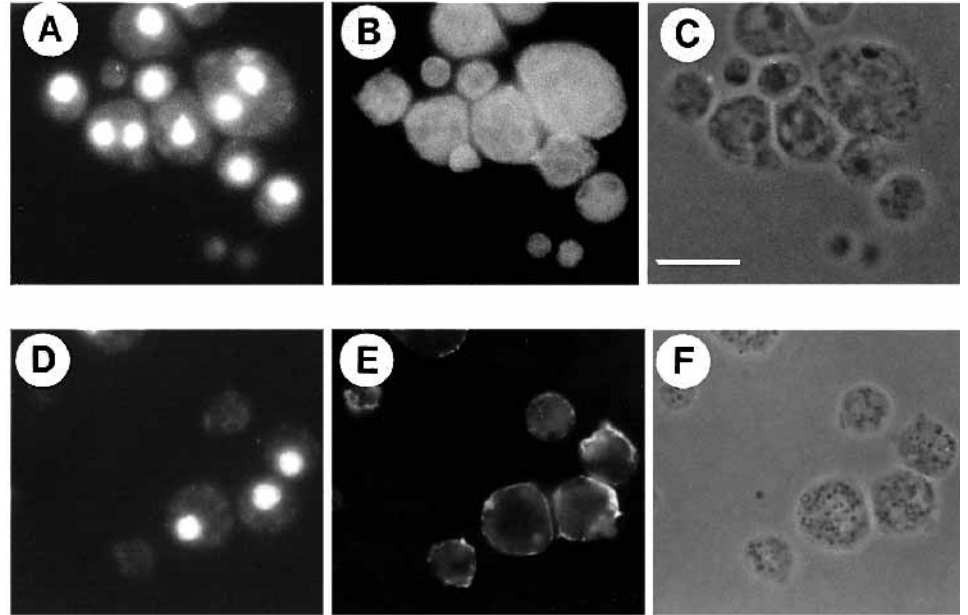
Fig. 3. Presence of nucleus free particles in strains AGHR2 and GHR. In AGHR2 (A-C) and GHR (D-F) cultures taken from shaken suspension, particles devoid of nuclei are frequently observed. In A and D the nuclei are visualized by staining with DAPI, in B the distribution of profilin I in AGHR2 as detected with mAb 153-246-10 (Haugwitz et al., 1991) and in E the actin distribution as detected with a monoclonal antibody (Simpson et al., 1984) are shown. (C, F) Phase contrast. Bar, 10 μm.

AGHR2 cells needed approximately 5 minutes to overcome similar distances.

For quantitative chemotactic analysis cells were analyzed in a chemotaxis chamber with a camera and subsequent computer analysis (Fisher et al., 1989). In the absence of cAMP wild-type strain AX2 exhibited an average speed of 7.1±2.9 μm/minute (Table 1). The lack of either α-actinin or gelation factor did not result in a significant change in speed compared to AX2. The double mutant strain AGHR2 in contrast was slower both in the absence and in the presence of cAMP. AGHR2-R cells which expressed the gelation factor after transformation with plasmid pHGE (see below) were indistinguishable from wild-type motility in the absence of cAMP. After applying a cAMP gradient double mutant AGHR2 failed to respond to the chemoattractant and orient in the direction of the gradient. The altered chemotactic behavior of AGHR2 was restored in the transformant AGHR2-R. The turning rate, which was calculated as the variance of direction changes between successive time-lapse intervals divided by the time-lapse interval, was comparable between all strains tested, suggesting that the lack of one or both actin-crosslinking proteins did not affect the frequency of turnings.

Cell shape of double mutants

A comparison of Fig. 7A,B and C,D shows that after starvation AGHR2 cells are more rounded than AX2 cells, which are elongated and polarized. Single mutants AHR and GHR were indistinguishable from AX2 in cell shape and actin distribution. The absence of cell shape changes in AGHR2 was also observed when cells were assayed in chemotaxis experiments and stimulated with a pipette filled with cAMP. Although cells were able to move towards the pipette albeit slowly, they did not assume the typical elongated cell shape as was observed for strains AX2, AHR and GHR. Moreover, we also noted that pseudopod formation was different from control and single mutants strains, which extended well formed broad pseudopods in the direction of the cAMP source. AGHR2 cells in contrast extended rather small pseudopods and these were frequently formed in positions pointing away from the chemotactic source. Further studies and quantitative analyses will be needed to characterize in more detail these observations.

Development of the double mutant strains

Upon starvation *D. discoideum* cells undergo a developmental cycle in which single amoebae aggregate to form a multicel-
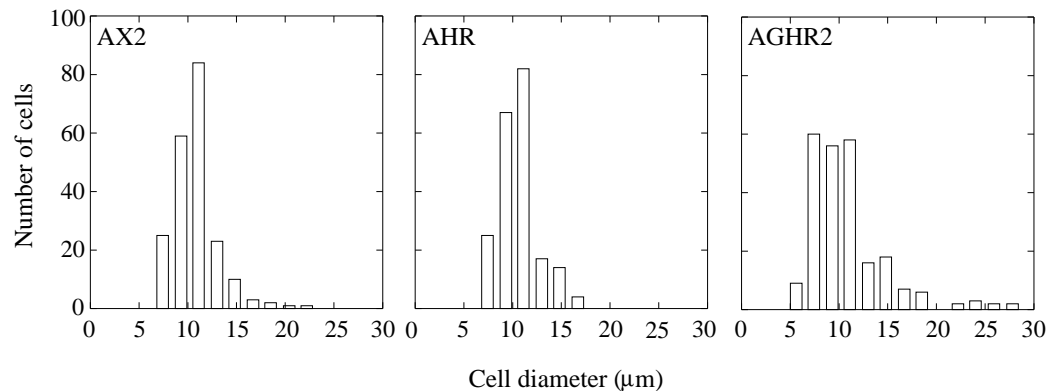

Fig. 4. Size histograms of AX2, AHR and AGHR2 cells. Single cells were photographed and the diameter for 200-250 cells per strain determined from the prints. For GHR cells a size distribution similar to that of AX2 and AHR was obtained.

Table 1. Motility of wild-type and mutant strains

Strain	N exp.	Speed [μm/min]		Orientation [cosθ]		Turning rate [rad^2/min]	
		Buffer	Gradient	Buffer	Gradient	Buffer	Gradient
AX2	6	7.1±2.9	10.7±2.1	0.02±0.11	0.23±0.08	2.0±0.5	1.7±0.9
GHR	3	5.6±2.3	8.3±0.5	0.09±0.12	0.14±0.03	1.2±0.3	1.5±0.1
AHR	3	10.2±5.9	11.6±3.1	0.08±0.10	0.11±0.06	1.3±0.3	1.6±0.4
AGHR2	4	3.8±1.8	7.3±1.6*	0.01±0.03	0.06±0.05*	2.2±0.6	1.3±0.2
AGHR2R	2	7.5±0.1	8.3±0.4	0.04±0.03	0.14±0.01	1.8±0.4	1.6±0.3

Cell tracks were recorded over four 30 minutes periods. In each period 41 images were taken with a time lapse of 45 seconds between subsequent images. During the first two half hours movement in buffer was analyzed, during the second two half hour periods a linear cAMP gradient with a steepness of 2.5×10^{-8} M cAMP/mm was applied. The values shown in the table were recorded in the first and third half hour period. In each period 50-80 individual cells were averaged. To avoid cells not only responding to the applied gradient but also to cAMP secreted by other cells, cell densities were used where the average distances between adjacent cells were at least 50 μm. Furthermore, care was taken that no cell aggregates were present. The orientation is expressed as cosθ, i.e. the higher the values the better the orientation in the gradient. Values are given as means ± s.d. *$P<0.05$ relative to AX2 (ANOVA).

lular fruiting body. This cycle involves differentiation into spore and stalk cells and requires the sequential expression of developmentally regulated genes. In strain AGHR2 development was heavily impaired. On phosphate agar plates AGHR2 cells were able to form long aggregation streams similar to that of AX2 wild-type cells (see Figs 10A,D and 12A). Later during aggregation many AGHR2 streams broke up, leading to the formation of small aggregates. Under these conditions tip and finger formation and occasionally short thick slugs could be observed, but no further development occurred (Fig. 8). Overall the developmental pattern of the double mutant cells was significantly delayed as compared to wild-type cells. The single mutants AHR and GHR usually formed smaller aggregation territories which also resulted in smaller mounds as compared to AX2 cells. Surprisingly both single mutants needed less time to form tipped aggregates. Furthermore they were able to complete development resulting in the formation of normal looking fruiting bodies.

Further investigations of AGHR2 showed that the stage at which development was blocked varied with the substrate used. When deposited on nitrocellulose filters AGHR2 cells

did not develop into aggregates. In parallel, mRNAs specific for the aggregation stage like contact site A message (Noegel et al., 1986) were not expressed or were present at reduced levels, as the mRNA corresponding to cAMP receptor cAR1 (Klein et al., 1988). The messages of genes later expressed in development such as the *D19* (Early et al., 1988), *ecmA* and *ecmB* genes (Jermyn et al., 1987) were not detected in strain AGHR2, suggesting that a differentiation into prespore and prestalk cells did not take place. During development on phosphate agar strain AGHR2 aggregated. cARI- as well as csA-specific RNA could be detected at 6 hours after beginning starvation, and at 18 hours the cell type specific mRNAs coding for PsA and EcmA and EcmB proteins were expressed. Whereas PsA and EcmA expression is comparable in AX2 and AGHR2, slightly lower levels of EcmB mRNA are apparent (Fig. 9). The expression of these markers did not substantially differ between strains AX2, AHR and GHR.

Starvation in suspension culture also allowed development of AGHR2 as determined by the presence of the aggregation specific csA protein, which is enriched at sites of cell to cell contact (Fig. 7B,D).
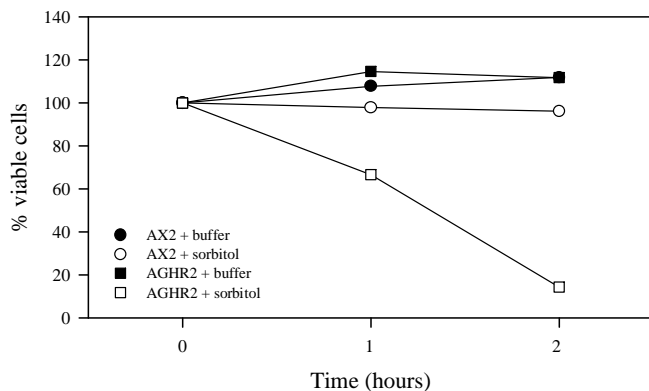

Fig. 5. Resistance to osmotic shock of strains AX2 and AGHR2. Cells were shaken in phosphate buffer in the presence or absence of 0.4 M sorbitol for the times indicated, diluted into phosphate buffer and plated onto SM agar plates with *K. aerogenes*. Cell viability after 1 or 2 hours of treatment was determined as the percentage of colonies in relation to 0 hours, which was assigned 100%. Each point is the average of colony counts from 5 plates. The results of one representative experiment are shown.
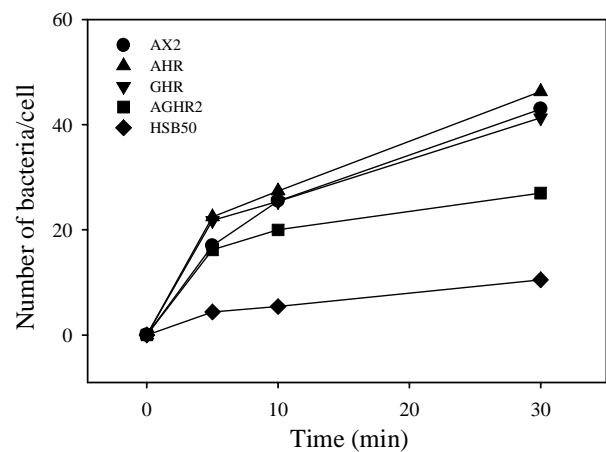

Fig. 6. Phagocytosis of bacteria by wild-type and mutant cells. Cells were incubated with FITC-labelled *E.coli* B/r under shaking conditions for the times indicated, and the number of cell-associated bacteria determined as described in Materials and Methods. Each point is the average of determinations made in triplicate. The results of one representative experiment are shown. Similar results were obtained in three independent experiments.
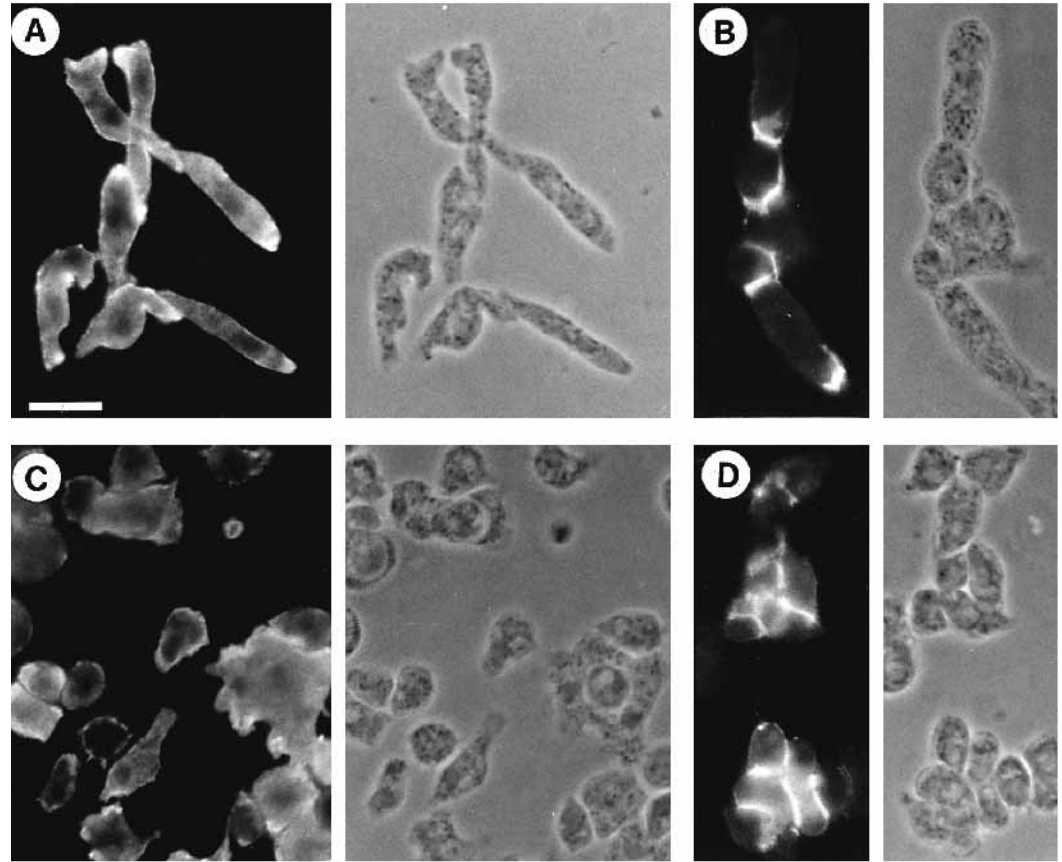
Fig. 7. Shape of aggregation competent AX2 (A,B) and AGHR2 (C,D) cells. Cells were starved in Soerensen phosphate buffer for 6 hours, fixed and stained with actin (A,C) or contact site A (B,D) specific monoclonal antibodies. For each panel immunofluorescence and phase contrast are shown. AGHR2 cells are unpolarized and do not show the typical elongated shape of AX2 cells. Bar, 10 µm.

Analysis of optical density wave propagation during aggregation and mound formation

As pointed out above development of the double mutant is blocked just after the tipped mound stage of development. Aggregation and mound formation result from relay of cAMP waves initiated by the aggregation center and chemotactic cell movement towards increasing cAMP gradients. The observed defects could result from both defects in signal generation and propagation as well as from defects in the chemotactic response.

Time lapse videos showed that wave propagation and rotational cell movement, both clockwise and counter clockwise, occur in aggregates of both the wild type and the double mutant strain. AHR and GHR formed small rotating mounds and rings. To visualize the spatial pattern of wave propagation an image-subtraction algorithm was used which resulted in white propagating waves on a dark background (Fig. 10B,E). Fig. 10B shows concentric ring waves emanating from the AX2 mound shown in Fig. 10A, whereas in Fig. 10E the pattern of wave propagation of the AGHR2 mound from Fig. 10D is a multi-
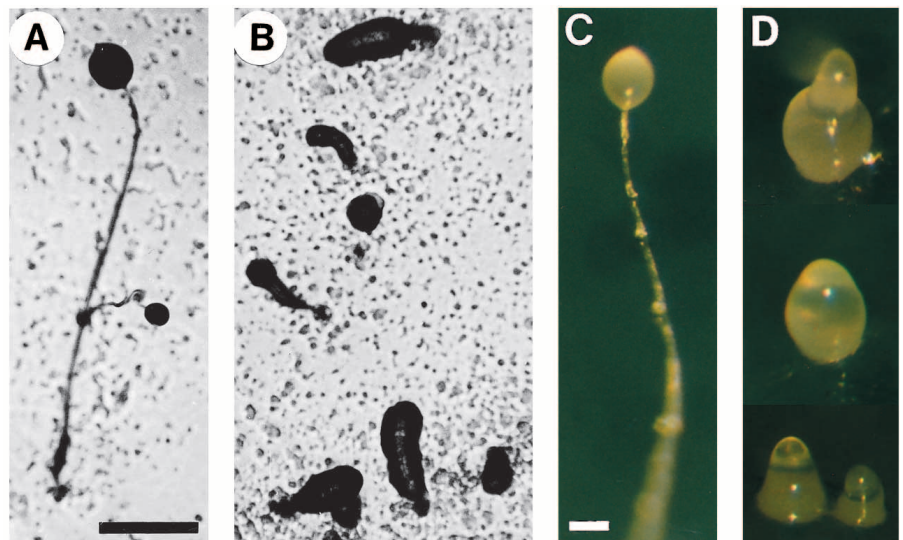

Fig. 8. Development of strains AX2 (A,C) and AGHR2 (B,D). Cells were plated either on nutrient agar on a lawn of *E. coli* B/2 (A,B) or on phosphate agar (C,D) and allowed to develop at 21°C. Pictures in C and D were taken 24 hours after plating the cells; no further development occurred. Bars: 0.5 mm for A and B; 0.1 mm for C and D.
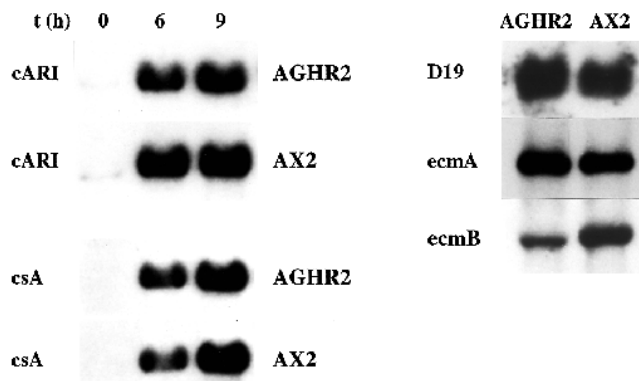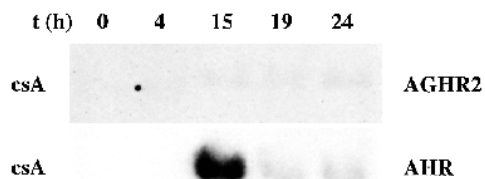
A. Development on phosphate agar

B. Development on filter

Fig. 9. Expression of developmentally regulated genes in strains AX2 and AGHR2 after development on phosphate agar (A) and nitrocellulose filters (B). Cells (1×10^8) were allowed to develop at 21°C and harvested at different time points (in hours) for RNA isolation; 10 µg of total RNA per time point were separated in formaldehyde agarose gels (1.2% agarose). After transfer onto nylon membranes the blots were hybridized with the indicated cDNAs. For expression of cell type specific genes, RNA isolated 18 hours after beginning starvation was probed with cell type specific cDNAs.

armed spiral rotating counterclockwise. Spiral and concentric patterns of wave propagation could be observed in all strains studied, although in the AHR and GHR mutants multiarmed spirals were more frequently observed.

To quantitate darkfield wave propagation we constructed time-space plots by measuring changes in the optical density along a cross-section of a mound (Siegert and Weijer, 1995). As an example of the method employed Fig. 10C,F shows typical time-space plots of AX2 (C) and AGHR2 (F) mounds at late stages of mound formation. Propagating waves appear as a pattern of alternating dark and bright bands. By plotting the intensity values versus time at a certain location in the mound the period length of darkfield waves can be determined by measuring the distance between the minima of gray values (Siegert and Weijer, 1989). We show two plots of temporal behavior for both AX2 (Fig. 10G,c) and AGHR2 (Fig. 10G,f) at a late stage of mound formation, corresponding to measurements made in Fig. 10C and F, respectively.

Fig. 11 summarizes the results of this analysis performed during mound formation in double and single mutants compared to wild-type AX2 cells. In aggregates of wild-type and single mutant cells, measurements could be started as soon as 5 hours after plating on KK2-agar, whereas in aggregates of AGHR2, which were significantly delayed in development, measurements

could be started approximately 7 hours after plating. In AX2 mounds the period length was found to be approximately 1.5 minutes at 7 hours of development and this period increased to 4-5 minutes just before tip formation. The double mutant showed significantly ($P<0.001$, ANOVA) longer periods of around 2 minutes at 7 hours of development. Later on, the periodicity increased up to 4-5 minutes, similar to AX2, and was maintained for very long periods of time. Both the AHR and GHR mutants showed similar period lengths in the range of 0.6-1.4 minutes between 5 and 7 hours of development, which are significantly lower ($P<0.001$, ANOVA) than that of AX2. After 7 hours both single mutants formed tips without measurable decrease in period length as in AX2 or the double mutant. These results suggest that the cAMP signalling system although not impaired, is altered in both the single as well as in the double mutants.

Analysis of cell movement of AGHR2 during mound formation

In order to be able to quantitatively compare the movement of double mutant with wild-type cells under conditions where they both respond to the same signals we perfomed synergy experiments between AX2 and AGHR2 cells (Fig. 12). A low percentage of AX2-gfp cells expressing green fluorescent protein was mixed with AGHR2 mutant cells, in which a low percentage of cells (0.3%) was labelled with rhodamine dextran and movement for both cell types recorded. Analysis of these experiments showed that AX2 cells moved significantly ($P<0.001$, Student's t-test) faster in chimeric aggregation streams (5.6 ± 1.9 µm/minute, $n=23$) than the rhodamine labelled AGHR2 cells (3.6 ± 1.6 µm/minute, $n=32$).
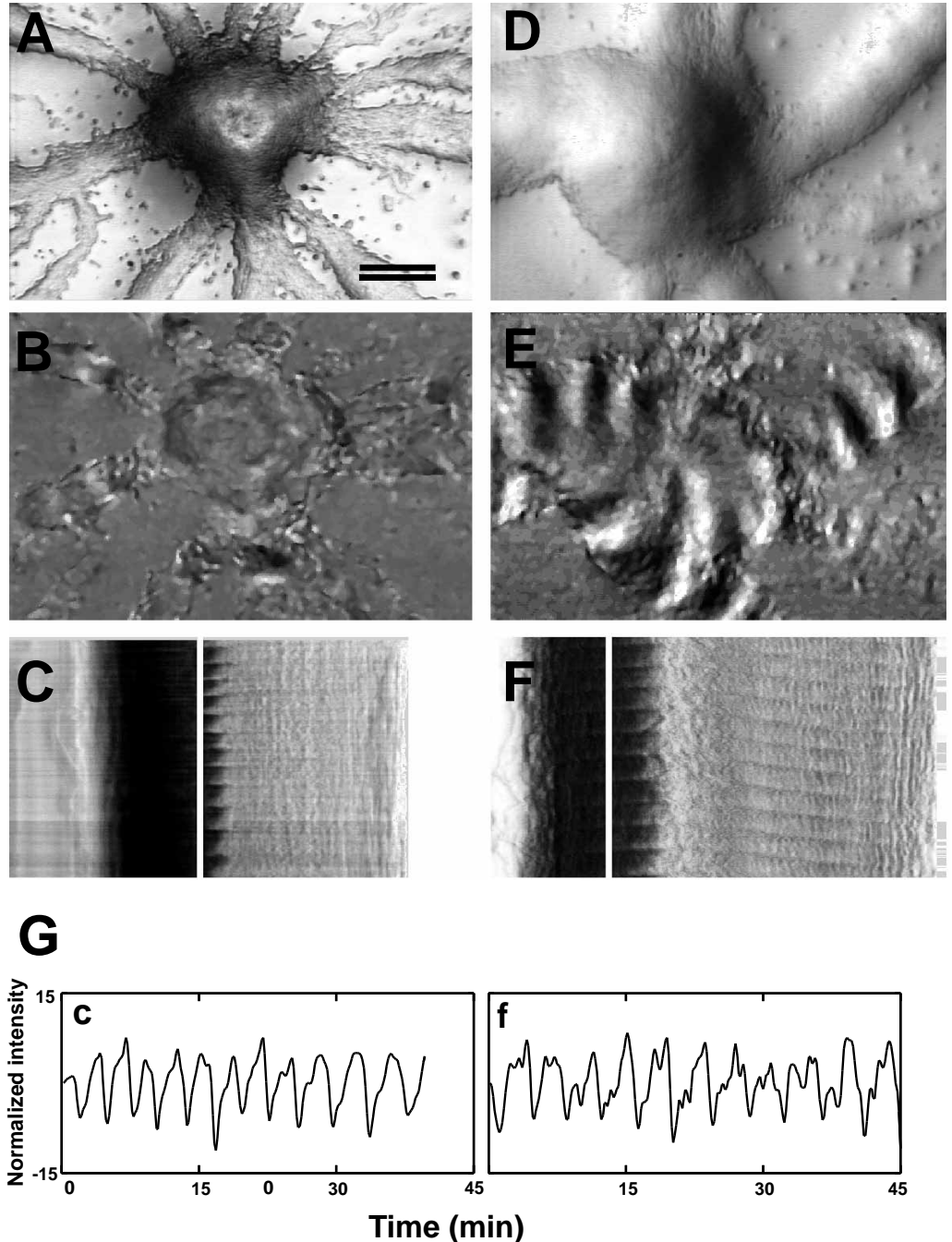
Contrary to AGHR2, in the course of aggregation the AX2 cells collected preferentially in the aggregation center (Fig. 12B,C). This was checked explicitly by performing synergy experiments between AGHR2 cells and AX2 cells expressing the reporter gene β-galactosidase under the control of the actin 6 promoter (Bichler and Weijer, 1994) and fixing the mounds at different times of development. The AX2 cells aggregated within the mound of AGHR2 cells and formed one or several centers (Fig. 12D). This situation persisted for 6 hours, then the AX2 cells dispersed again.

Rescue of mutant AGHR2 by expression of gelation factor

AGHR2 was transformed with plasmid pHGE that harbored the gelation factor cDNA under the control of the actin 15 promoter and actin 8 terminator. Transformants were selected for expression of the protein and development was analyzed. Western blot analysis revealed that the 120 kDa gelation factor was expressed with similar levels as in AX2 wild type (Fig. 13A) and by Southern blot analysis a single copy integration into the gelation factor gene was detected leading to stable expression of the protein. All clones expressing the 120 kDa gelation factor formed fruiting bodies (Fig. 13B).

DISCUSSION

Alterations in cell size, growth and sensitivity to osmotic shock

Cells lacking α-actinin and gelation factor exhibit several defects already during growth, the most notable being a reduced growth rate, a reduction in cell size and increased sensitivity

Fig. 10. Wave propagation in AX2 and AGHR2 mounds. (A,D) Dark field images of AX2 (A) and AGHR2 (D) early mounds on KK2-agar. (B,E) Wave propagation in AX2 (B) and AGHR2 (E) mounds shown in A and D, respectively, visualized by image subtraction. Two images 25 seconds apart were subtracted; this resulted in bright pixel values where the two images differ and dark values where the two images are identical or similar. In B wave propagation is concentric, whereas in E wave propagation appears as a multiarmed spiral. (C,F) Time-space plots of wave propagation in AX2 (C) and AGHR2 (F) late mounds. Time-space plots were constructed as described in Materials and Methods. Recording was started 8 (C) and 13 (F) hours after plating the cells. Images were taken every 10 seconds. The number of images recorded was 270. (G) Oscillatory pattern in AX2 (c) and AGHR2 (f) mounds analyzed from time-space plots C and F, respectively. Each graph was obtained by plotting the normalized and frequency filtered intensity values along the vertical line shown in the corresponding time-space plot. Bar, 100 μm.

towards osmotic shock. These altered properties could well reflect a reduced strength of the cortical cytoskeleton which cannot resist the internal forces during cell growth and leads to a much smaller cell size. There exists also a population (about 5%) of very large multinucleated cells suggesting that both crosslinking proteins might be involved in the division of daughter cells after DNA replication. In this respect AGHR2 cells resemble *D. discoideum* cells deficient in myosin II (De Lozanne and Spudich, 1987; Manstein et al., 1989; Pollenz et al., 1992), profilin (Haugwitz et al., 1994) or coronin, an actin-binding protein preferentially found in crown-like cell surface protrusions of *D. discoideum* (De Hostos et al., 1991, 1993). Lack of these proteins resulted in a defect in cytokinesis leading to large multinucleated cells. The effects were, however, much more pronounced than in double mutant cells. Generation of multinucleated cells in general indicates impaired cytokinesis although there have been no indications from immunofluores-cence studies that the crosslinkers are located in the cleavage furrow as was shown for myosin II (Yumura et al., 1984) and would strongly support a role in cytokinesis.

Most remarkable is the formation of particles of considerable size but without a nucleus. These particles were already observed in the GHR mutant lacking only the gelation factor. They could be generated by a mechanism that has been suggested for the formation of blebs. In general blebs as surface extensions are thought to be generated by fluid driven expansion
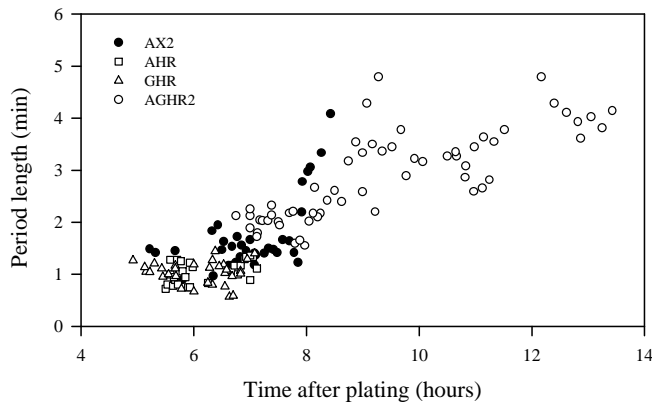
Fig. 11. Analysis of period length of darkfield waves during mound formation in single (AHR, GHR) and double (AGHR2) mutants as compared to AX2. Periodicity was determined from graphs derived from time-space plots, similar to those shown in Fig. 10G. The distance between the minima of the gray values was measured. For each data point 4 to 6 successive waves were averaged. The number of mounds analyzed was 13 (AX2), 20 (AGHR2), 6 (AHR) and 13 (GHR). Mounds were recorded for 15 to 80 minutes.

of the cell membrane (Cunningham, 1995). The expansion decreases as cortical gelation is achieved. This model is based on data obtained with cells lacking ABP280. The cells showed an extensive surface blebbing which could be suppressed by the introduction of ABP280 (Cunningham et al., 1992). The gelation factor is very similar to ABP280 with regard to primary and secondary structure and our data suggest that it is also involved in this particular aspect of the cortical cytoskeleton. An impaired cytokinesis together with the formation of non-nucleated particles might well be responsible for the reduced growth rate of double mutant cells in shaking culture.

The increased sensitivity in double mutant cells to osmotic shock is also in agreement with a reduced strength of the cortical

cytoskeleton. There is increasing evidence indicating that the actin cytoskeleton plays an important role in the adaptation to situations of altered tonicity. In a recent study it has been observed that melanoma cells deficient in ABP280 are not able to activate potassium channels and to regulate their volume when swollen in diluted solutions. Rescue of the cells by transfection with ABP280 corrected these defects (Cantiello et al., 1993). In yeast a rapid and reversible disassembly and redistribution of the actin cytoskeleton occurs in response to an osmotic stress, and genetic and morphological studies performed with osmosensitive mutants indicate that an actin-binding protein could be involved in actin redistribution during osmotic shock (Chowdbury et al., 1992). *Dictyostelium* responds to an osmotic stress by a relocalization of myosin which allows the cells to adopt a spherical shape and provides the mechanical strength necessary to resist extensive shrinkage (Kuwayama et al., 1996). These reports along with the results reported here point to an interplay of the various components of the actin cytoskeleton in response to osmotic stress whose details remain to be elucidated.

Alterations in phagocytosis

Besides actin, a variety of actin-binding proteins have been shown to be involved in phagocytosis in *Dictyostelium discoideum*. Whereas coronin (Maniak et al., 1995), myosin IB (Fukui et al., 1989), the 30 kDa actin-bundling protein (Furukawa and Fechheimer, 1994) and gelation factor (Cox et al., 1996) colocalize with actin at the phagocytic cup at the onset of phagocytosis, immunofluorescence studies suggest that α-actinin is involved in later stages (Furukawa and Fechheimer, 1994). Lack of either α-actinin or gelation factor did not result in alterations of the rate of phagocytosis; on the contrary, double mutants lacking both crosslinkers showed a reduction of about 50% in the rate of phagocytosis. Our data also suggest that early steps of phagocytosis are not affected in double mutants, pointing out a differential contribution of both crosslinkers to the diverse phases of phagocytosis. As shown by the analysis of mutants deficient

Fig. 12. Movement of AX2-gfp cells in aggregates of AGHR2. (A) Transmitted light image of a late AGHR2 aggregate (8 hours of development). Bar, 150 μm. (B) Fluorescence image of the same aggregate as in A, showing the localization of few (0.3%) AX2-gfp cells in the mound. (C) Fluorescence image of the same mound 30 seconds later than the one in B showing distribution and shape of AGHR2 cells, which were labelled with rhodamine-dextran. (D) Synergy experiment with 99% AGHR2 cells and 1% AX2-gal cells after 17 hours of development. The AX2-gal cells have preferentially accumulated in the center of the mound. Bar, 50 μm.
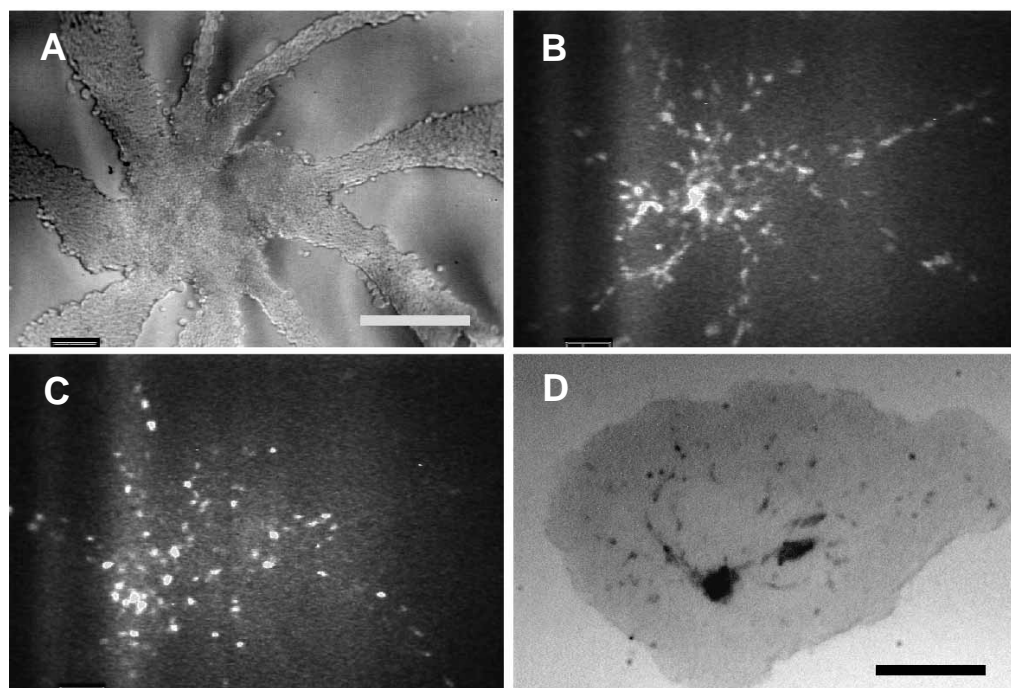
A

B

Fig. 13. Rescue of AGHR2 by introduction of a gelation factor expression vector. AGHR2 cells were transformed with the expression vector pHGE and transformants expressing 120 kDa gelation factor were tested for the ability to form fruiting bodies. (A) Total cell protein of 2×10^5 cells of strain AX2 (lane 1), AGHR2 (lane 2) and transformant AGHR2-R (lane 3) was separated by SDS-PAGE, transferred onto nitrocellulose and incubated with the gelation factor specific mAb 82-471-17. (B) AGHR2-R cells expressing gelation factor were allowed to develop at 21°C on nutrient agar plates on a lawn of *E. coli* B/2. Bar, 1 mm.
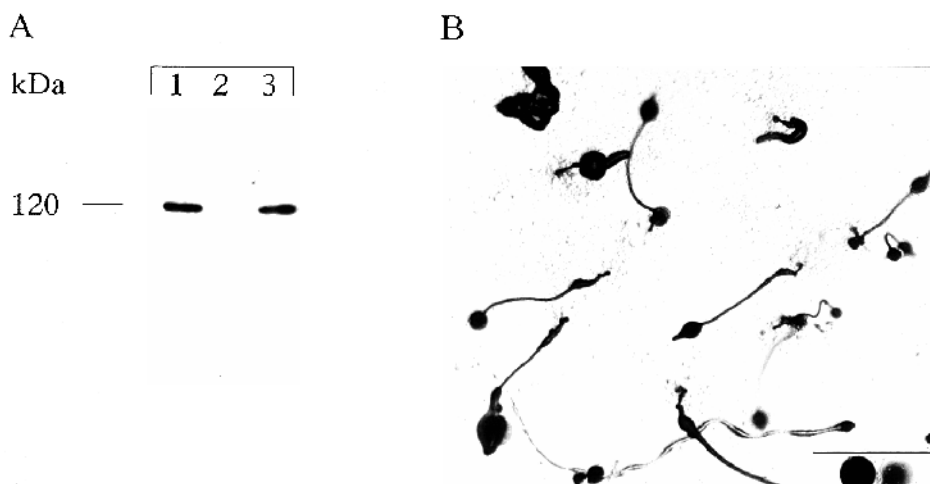
in cytoskeletal proteins, the contribution of these proteins to phagocytosis is variable. In mutants defective in coronin or myosin IB the rate of phagocytosis is reduced by about 70% or 30%, respectively (Maniak et al., 1995; Jung and Hammer, 1990), whereas mutants deficient in 30 kDa actin-bundling protein are unimpaired in phagocytosis (Rivero et al., 1996). In contrast to our results mutant strains deficient in gelation factor generated by Cox et al. (1996) show a 50% reduction in the ability to phagocytose bacteria. These differences might be explained by the different *Dictyostelium* parent strains used, AX2 for GHR and AX3 (Cox et al., 1992, 1996).

Alterations in chemotaxis

After stimulation with cAMP the cortical actin cytoskeleton undergoes a dramatic reorganization which leads to a change in the direction of new pseudopod extension and consequently in the direction of cell locomotion. Actin crosslinking proteins are thought to be essential in this process since they allow the stabilization of the newly formed structures. A loss of actin crosslinking proteins should result in the formation of less stable protrusions and lead to impaired cell locomotion (Condeelis, 1993). When assayed in a chemotactic chamber cells lacking either α-actinin or gelation factor did not exhibit significant differences in velocity compared to wild-type cells. This is in agreement with motility data obtained with chemically derived mutant strains (Brink et al., 1990; Schleicher et al., 1988; Wallraff et al., 1986). A gelation factor defective strain has been described by Cox et al. (1992). Characterization of this strain suggested that the lack of gelation factor resulted in abnormalities in the rate and extent of pseudopod formation and also in the amount of F-actin incorporated into newly formed pseudopods after stimulation with chemoattractant. Furthermore, cells expressing no gelation factor were roughly three times slower than wild-type cells when moving in buffer and also exhibited altered motility 20-40 seconds after stimulation with cAMP. As was the case also for phagocytosis defects, these differences in cell motility between the ABP-120⁻ strains generated by Cox et al. (1992, 1996) and the strain generated by Brink et al. (1990) and the strain GHR described here might be explained by the different *Dictyostelium* parent strains used.

In contrast to mutant strains AHR and GHR, the speed of double mutant cells was reduced by more than 30% both in the

absence and presence of cAMP. The defect could be restored by expression of gelation factor in the transformant AGHR2-R. Furthermore, double mutant strain AGHR2 was not able to orient properly in a chemotactic gradient and move towards the cAMP source. This result contrasts with the fact that in the micropipette assay AGHR2 cells moved towards a pipette filled with cAMP although with a reduced speed and abnormal pseudopod formation. In this respect it has to be considered that the motility assay performed in the chemotaxis chamber and the assay performed with the micropipette differ in the concentrations of cAMP, although an effect of the different substrates used in each case (BSA coated glass in the chemotaxis chamber and uncoated glass in the micropipette assays) cannot be excluded. Indeed, the formation of reversible substrate adhesion sites is an essential aspect of cell locomotion (Stossel, 1993). In addition, cells were capable of streaming and aggregating when deposited on agar plates indicating a production of and a response to cAMP.

The analysis of cell movement in chimeric streams constituted by AGHR2 cells and a low percentage of fluorescently labelled AGHR2 and AX2 cells clearly shows that AGHR2 cells are much more rounded and unpolarized than AX2 cells, being in agreement with observations made in the micropipette assay and in immunofluorescence studies. A less polarized cell shape has been observed in aggregating myosin heavy chain (MHC) minus cells as well (Eliott et al., 1993). Furthermore MHC minus cells like AGHR cells exhibited less directed and coordinated movements in streams (Doolittle et al., 1995). From our cell movement analysis it also becomes clear that the double mutant cells move less efficiently than AX2 towards the same in vivo signals.

Alterations in development

Whereas mutants lacking one of the two actin crosslinking proteins are able to aggregate and make normal looking fruiting bodies, mutants lacking both proteins have a developmental defect and do not appreciably form fruiting bodies. In this respect AGHR2 cells resembled the previously described double mutants (GA and AG series; Witke et al., 1992) in their inability to undergo the complete developmental cycle. In contrast to the GA and AG strains which, depending on the conditions, occasionally formed fruiting bodies, no fruiting body formation was detectable for strains AGHR2 and AGHR1 under

all conditions tested. When deposited on nitrocellulose filters the block occurred at a much earlier stage of development compared to GA mutants and abolished the ability of AGHR2 cells to differentiate into prespore and prestalk cells whereas in GA cells the expression pattern of early and late genes was comparable to the one of wild-type cells, including a differentiation into prespore and prestalk cells. These differences could be due to the nitrosoguanidine treatment of the GA parents which could have affected other loci resulting in a partial rescue of the phenotype. This could also explain the different behavior of AGHR2 and the previously described strains in cell growth and phagocytosis. During development on phosphate-buffered agar AGHR2 cells were able to aggregate, but development stopped at the mound stage just after the formation of the tip. RNA analyses have shown that a differentiation into prestalk and prespore cells takes place in AGHR2 cells. A substrate dependent adhesion could account for the different developmental pattern observed on nitrocellulose filters and on agar.

The analysis of optical density wave propagation allowed us to study the chemotactic signal relay which controls aggregation and mound formation. Our measurements of optical density wave propagation show that the mutant is capable of generating the characteristic increase in signal period length during aggregation, reaching periods below two minutes followed by a characteristic lengthening to 4-5 minutes just before tip formation. This increase in period length has been attributed to a switch from high to low affinity cAMP receptors (Rietdorf et al., 1996). Therefore the double mutants seem to be able to express these types of receptors to levels sufficient for a physiological relevant response.

Synergy experiments show that the mutant cells are able to generate the signals required for tip formation, but are not able to sort properly. Even if in mutant and wild-type mixtures AX2 cells collect in the tip and presumably generate suitable signals for tip formation AGHR2 cells cannot respond properly. The situation partially resembles that found with MHC minus mutants, which can differentiate but cannot sort out to form a tip (Springer et al., 1994; Traynor et al., 1994; Doolittle et al., 1995; Shelden and Knecht, 1995). This deficiency has been attributed to a reduced tactile strength during aggregation and mound stage (Wessels et al., 1991; Shelden and Knecht, 1995). Thus, in both situations, the one reported here and in myosin minus cells, a weakened cortical cytoskeleton might not allow cells to generate the protrusive force necessary to migrate and sort out within a mass of aggregated cells.

REFERENCES

André, E., Brink, M., Gerisch, G., Isenberg, G., Noegel, A. A., Schleicher, M., Segall, J. E. and Wallraff, E. (1989). A *Dictyostelium* mutant deficient in severin, an F-actin fragmenting protein shows normal motility and chemotaxis. *J. Cell Biol.* **108**, 985-995.

Berthold, J., Stadler, J., Bozzaro, S., Fichtner, B. and Gerisch, G. (1985). Carbohydrate and other epitopes of the contact site A glycoprotein of *Dictyostelium discoideum* as characterized by monoclonal antibodies. *Cell Differ.* **16**, 187-202.

Bichler, G. and Weijer, C. J. (1994). A *Dictyostelium* anterior-like cell mutant reveals sequential steps in the prespore prestalk differentiation pathway. *Development* **120**, 2857-2868.

Bozzaro, S., Merkl, R. and Gerisch, G. (1987). Cell adhesion: its quantification, assay of the molecules involved and selection of defective mutants in *Dictyostelium* and *Polysphondylium*. *Meth. Cell Biol.* **28**, 359-385

Brink, M., Gerisch, G., Isenberg, G., Noegel, A. A., Segall, J. E., Wallraff, E. and Schleicher, M. (1990). A *Dictyostelium* mutant lacking an F-actin cross-linking protein, the 120-kD gelation factor. *J. Cell Biol.* **111**, 1477-1489.

Cantiello, H. F., Prat, A. G., Bonventre, J. V., Cunningham, C. C., Hartwig, J. H. and Ausiello, D. A. (1993). Actin-binding protein contributes to cell volume regulatory ion channel activation in melanoma cells. *J. Biol. Chem.* **268**, 4596-4599.

Ceccarelli, A. and Bozzaro, S. (1992). Selection of mutants defective in binding to immobilized carbohydrates in *Dictyostelium discoideum*. *Animal Biology* **1**, 50-68.

Chowdbury, S., Smith, K. W. and Gustin, M. C. (1992). Osmotic stress and the yeast cytoskeleton: phenotype specific suppression of an actin mutation. *J. Cell Biol.* **118**, 561-571.

Claviez, M., Pagh, K., Maruta, H., Baltes, W., Fisher, P. and Gerisch, G. (1982). Electron microscopic mapping of monoclonal antibodies on the tail region of *Dictyostelium* myosin. *EMBO J.* **1**, 1017-1022.

Condeelis, J., Hall, A., Bresnick, A., Warren, V., Hock, R., Bennett, H. and Ogihara, S. (1988). Actin polymerization and pseudopod extension during amoeboid chemotaxis. *Cell Motil. Cytoskel.* **10**, 77-90.

Condeelis, J. (1993). Understanding the cortex of crawling cells: Insights from *Dictyostelium*. *Trends Cell Biol.* **3**, 371-376.

Cox, D., Condeelis, J., Wessels, D., Soll, D., Kern, H. and Knecht D. A. (1992). Targeted disruption of the ABP-120 gene leads to cells with altered motility. *J. Cell Biol.* **116**, 943-955.

Cox, D., Wessels, D., Soll, D. R., Hartwig, J. and Condeelis, J. (1996). Re-expression of ABP-120 rescues cytoskeletal, motility, and phagocytosis defects of ABP-120⁻ *Dictyostelium* mutants. *Mol. Biol. Cell* **7**, 803-823.

Cunningham, C. C., Gorlin, J. D., Kwiatkowski, D. J., Hartwig, J. H., Janmey, P. A., Byers, H. R. and Stossel T. P. (1992). Actin-binding protein requirement for cortical stability and efficient locomotion. *Science* **255**, 325-327.

Cunningham, C. C. (1995). Actin polymerization and intracellular solvent flow in cell surface blebbing. *J. Cell Biol.* **129**, 1589-1599.

De Hostos, E. L., Bradtke, B., Lottspeich, F., Guggenheim, R. and Gerisch, G. (1991). Coronin, an actin-binding protein of *Dictyostelium discoideum* localized to cell surface projections, has sequence similarities to G protein β subunits. *EMBO J.* **10**, 4097-4104.

De Hostos, E. L., Rehfueß, C., Bradtke, B., Waddell, D. R., Albrecht, R., Murphy, J. and Gerisch, G. (1993). *Dictyostelium* mutants lacking the cytoskeletal protein coronin are defective in cytokinesis and cell motility. *J. Cell Biol.* **120**, 163-173.

De Lozanne, A. and Spudich, J. A. (1987). Disruption of the *Dictyostelium* myosin heavy chain gene by homologous recombination. *Science* **236**, 1086-1091.

Dingermann, T., Reindl, N., Werner, H., Hildebrandt, M., Nellen, W., Harwood, A., Williams, J. and Nerke, K. (1989). Optimization and in situ detection of *Escherichia coli* beta-galactosidase gene expression in *Dictyostelium discoideum*. *Gene* **85**, 353-362.

Doolittle, K. W., Reddy, I. and McNally, J. G. (1995). 3D analysis of cell movement during normal and myosin-II-null cell morphogenesis in *Dictyostelium*. *Dev. Biol.* **167**, 118-129.

Early, A. E., Williams, J. G., Meyer, H. E., Por, S. B., Smith, E., Williams, K. L. and Gooley, A. A. (1988). Structural characterization of *Dictyostelium discoideum* prespore-specific gene D19 and of its product, cell surface glycoprotein PsA. *Mol. Cell. Biol.* **8**, 3458-3466.

Egelhoff, T. T., Brown, S. S., Manstein, D. J. and Spudich, J. A. (1989). Hygromycin resistance as a selectable marker in *Dictyostelium*. *Mol. Cell. Biol.* **9**, 1965-1972.

Eichinger, L., Köppel, B., Noegel, A. A., Schleicher, M., Schliwa, M., Weijer, C. J., Witke, W. and Janmey, P. A. (1996). Mechanical perturbation elicits a phenotypic difference between *Dictyostelium* wild-type cells and cytoskeletal mutants. *Biophys. J.* **70**, 1054-1060.

Eliott, S., Joss, G. H., Spudich, A. and Williams, K. L. (1993). Patterns in *Dictyostelium discoideum*: the role of myosin II in the transition from the unicellular to the multicellular phase. *J. Cell Sci.* **104**, 457-466.

Faix, J., Gerisch, G. and Noegel, A. A. (1992). Overexpression of the csA cell

adhesion molecule under its own cAMP-regulated promoter impairs morphogenesis in *Dictyostelium discoideum. J. Cell Sci.* **102**, 203-214.

Fisher, P. R., Merkl, R. and Gerisch, G. (1989). Quantitative analysis of cell motility and chemotaxis in *Dictyostelium discoideum* by using an image processing system and a novel chemotaxis chamber providing stationary chemical gradients. *J. Cell Biol.* **108**, 973-984.

Fukui, Y., Lynch, T. J., Brzeska, H. and Korn, E. D. (1989). Myosin I is located at the leading edges of locomoting *Dictyostelium* amoebae. *Nature* **341**, 328-331.

Furukawa, R. and Fechheimer, M. (1994). Differential localization of α-actinin and the 30 kD actin-bundling protein in the cleavage furrrow, phagocytic cup, and contractile vacuole of *Dictyostelium discoideum. Cell Motil. Cytoskel.* **29**, 46-56.

Gerisch, G. and Keller, H. U. (1981). Chemotactic reorientation of granulocytes stimulated with micropipettes containing fMet-Leu-Phe. *J. Cell Sci.* **52**, 1-10.

Hartmann, H., Noegel, A. A., Eckerskorn, C., Rapp, S. and Schleicher, M. (1989). Ca^{2+} independent F-actin capping proteins: Cap32/34, a capping protein from *Dictyostelium discoideum*, does not share sequence homologies with known capping proteins. *J. Biol. Chem.* **264**, 12639-12647.

Haugwitz, M., Noegel, A. A., Rieger, D., Lottspeich, F. and Schleicher, M. (1991). *Dictyostelium discoideum* contains two profilin isoforms that differ in structure and function. *J. Cell Sci.* **100**, 481-489.

Haugwitz, M., Noegel, A. A., Karakesisoglou, J. and Schleicher, M. (1994). *Dictyostelium* amoebae that lack G-actin-sequestering profilins show defects in F-actin content, cytokinesis, and development. *Cell* **79**, 303-314.

Janssen, K.-P., Eichinger, L., Janmey, P., Noegel, A. A., Schliwa, M., Witke, W. and Schleicher, M. (1996). Viscoelastic properties of F-actin solutions in the presence of normal and mutated actin-binding proteins. *Arch. Biochem. Biophys.* **325**, 183-189.

Jermyn, K. A., Berks, M., Kay, R. R. and Williams, J. E. (1987). Two distinct classes of prestalk-enriched mRNA sequences in *Dictyostelium discoideum. Development* **100**, 745-755.

Jung, G. and Hammer, J. A. (1990). Generation and characterization of *Dictyostelium* cells deficient in a myosin I heavy chain isoform. *J. Cell Biol.* **110**, 1955-1964.

Klein, P. S., Sun, T. J., Saxe III, C. L., Kimmel, A. R., Johnson, R. L. and Devreotes, P. N. (1988). A chemoattractant receptor controls development in *Dictyostelium discoideum. Science* **241**, 1467-1472.

Knecht, D. A., Cohen, S. M., Loomis, W. F. and Lodish, H. F. (1986). Developmental regulation of *Dictyostelium discoideum* actin gene fusions carried on low-copy and high-copy transformation vectors. *Mol. Cell. Biol.* **6**, 3973-3983.

Kuwayama, H., Ecke, M., Gerisch, G. and Van Haastert, P. (1996). Protection against osmotic stress by cGMP mediated myosin phosphorylation. *Science* **271**, 207-209.

Kwon, H. M. and Handler, J. S. (1995). Cell volume regulated transporters of compatible osmolytes. *Curr. Opin. Cell Biol.* **7**, 465-471.

Laemmli, U. K. (1970). Cleavage of structural proteins during the assembly of the head of bacteriophage T4. *Nature* **227**, 680-685.

Luby-Phelps, K. (1994). Physical properties of cytoplasm. *Curr. Opin. Cell Biol.* **6**, 3-9.

Maniak, M., Rauchenberger, R., Albrecht, R., Murphy, J. and Gerisch, G. (1995). Coronin involved in phagocytosis: dynamics of particle-induced relocalization visualized by a green fluorescent protein tag. *Cell* **83**, 915-924.

Manstein, D. J., Titus, M. A., De Lozanne, A. and Spudich, J. A. (1989). Gene replacement in *Dictyostelium*: generation of myosin null mutants. *EMBO J.* **8**, 923-932.

Matsudaira, P. (1991). Modular organization of actin crosslinking proteins. *Trends Biochem. Sci.* **16**, 87-92.

Newell, P. C., Telser, A. and Sussman, M. (1969). Alternative developmental pathways determined by environmental conditions in the cellular slime mould *Dictyostelium discoideum. J. Bacteriol.* **100**, 763-768.

Noegel, A. A., Harloff, C., Hirth, P., Merkl, R., Modersitzki, M., Stadler, J., Weinhart, U., Westphal, M. and Gerisch, G. (1985). Probing an adhesion mutant of *Dictyostelium discoideum* with cDNA clones and monoclonal antibodies indicates a specific defect in the contact site A glycoprotein. *EMBO J.* **4**, 3805-3810.

Noegel, A. A., Gerisch, G., Stadler, J. and Westphal, M. (1986). Complete sequence and transcript regulation of a cell adhesion protein from aggregating *Dictyostelium* cells. *EMBO J.* **5**, 1473-1476.

Noegel, A. A., Rapp, S., Lottspeich, F., Schleicher, M. and Stewart, M. (1989). The *Dictyostelium* gelation factor shares a putative actin binding site with α-

actinins and dystrophin and also has a rod domain containing six 100-residue motifs that appear to have a cross-beta conformation. *J. Cell Biol.* **109**, 607-618.

Pollenz, R. S., Chen, T.-L. L., Trivinos-Lagos, L. and Chisholm, R. L. (1992). The *Dictyostelium* essential light chain is required for myosin function. *Cell* **69**, 951-962.

Rietdorf, J., Siegert, F. and Weijer, C. J. (1996). Analysis of optical density wave propagation and cell movement during mound formation in *Dictyostelium discoideum. Dev. Biol.* **177**, 427-438.

Rivero, F., Furukawa, R., Noegel, A. A. and Fechheimer, M. (1996). *Dictyostelium discoideum* cells lacking the 34,000 Dalton actin binding protein can grow, locomote and develop, but exhibit defects in regulation of cell structure and movement: A case of partial redundancy. *J. Cell Biol.* (in press).

Schleicher, M., Noegel, A. A., Schwarz, T., Wallraff, E., Brink, M., Faix, J., Gerisch, G. and Isenberg, G. (1988). A *Dictyostelium* mutant with severe defects in α-actinin: Its characterization by cDNA probes and monoclonal antibodies. *J. Cell Sci.* **90**, 59-71.

Schleicher, M., André, B., Andréoli, C., Eichinger, L., Haugwitz, M., Hofmann, A., Karakesisoglou, J., Stöckelhuber, M. and Noegel, A. A. (1995). Structure/function studies on cytoskeletal proteins in *Dictyostelium* amoebae as a paradigm. *FEBS Lett.* **369**, 38-42.

Segall, J. E., Fisher, P. R. and Gerisch, G. (1987). Selection of chemotaxis mutants of *Dictyostelium discoideum. J. Cell Biol.* **10**, 151-161.

Shelden, E. and Knecht, D. A. (1995). Mutants lacking myosin II cannot resist forces generated during multicellular morphogenesis. *J. Cell Sci.* **108**, 1105-1115.

Siegert, F. and Weijer, C. (1989). Digital image processing of optical density wave propagation in *Dictyostelium discoideum* and analysis of the effects of caffeine and ammonia. *J. Cell Sci.* **93**, 325-335.

Siegert, F. and Weijer, C. J. (1992). Three-dimensional scroll waves organize *Dictyostelium* slugs. *Proc. Nat. Acad. Sci. USA* **89**, 6433-6437.

Siegert, F. and Weijer, C. (1995). Spiral and concentric waves organize multicellular *Dictyostelium* mounds. *Curr. Biol.* **5**, 937-943.

Simpson, P. A., Spudich, J. A. and Parham, P. (1984). Monoclonal antibodies prepared against *Dictyostelium* actin: characterization and interaction with actin. *J. Cell Biol.* **99**, 287-295.

Springer, M. L., Patterson, B. and Spudich, J. A. (1994). Stage specific requirement for myosin II during *Dictyostelium* development. *Development* **120**, 2651-2660.

Stossel, T. P. (1993). On the crawling of animal cells. *Science* **260**, 1086-1094.

Traynor, D., Tasaka, M., Takeuchi, I. and Williams, J. (1994). Aberrant pattern formation in myosin heavy chain mutants of *Dictyostelium. Development* **120**, 591-601.

Vogel, G. (1987). Endocytosis and recognition mechanisms in *Dictyostelium discoideum. Meth. Cell Biol.* **28**, 129-138.

Wachsstock, D. H., Schwarz, W. H. and Pollard, T. D. (1994). Cross-linker dynamics determine the mechanical properties of actin gels. *Biophys. J.* **66**, 801-809.

Wallraff, E., Schleicher, M., Modersitzki, M., Rieger, D., Isenberg, G. and Gerisch, G. (1986). Selection of *Dictyostelium* mutants defective in cytoskeletal proteins: Use of an antibody that binds to the ends of α-actinin rods. *EMBO J.* **5**, 61-67.

Weiner, O. H., Murphy, J., Griffiths, G., Schleicher, M. and Noegel, A. A. (1993). The actin-binding protein comitin (p24) is a component of the Golgi apparatus. *J. Cell Biol.* **123**, 23-34.

Wessels, D., Soll, D. R., Knecht, D. A., Loomis, W. F., De Lozanne, A. and Spudich, J. A. (1988). Cell motility and chemotaxis in *Dictyostelium* amebae lacking myosin heavy chain. *Dev. Biol.* **128**, 164-177.

Williams, K. L. and Newell, P. C. (1976). A genetic study of aggregation in the cellular slime mould *Dictyostelium discoideum* using complementation analysis. *Genetics* **82**, 287-307.

Witke, W., Nellen, W. and Noegel, A. A. (1987). Homologous recombination in the *Dictyostelium* α-actinin gene leads to an altered mRNA and lack of the protein. *EMBO J.* **6**, 4143-4148.

Witke, W., Schleicher, M. and Noegel, A. A. (1992). Redundancy in the microfilament system: Abnormal development of *Dictyostelium* cells lacking two F-actin crosslinking proteins. *Cell* **68**, 53-62.

Yumura, S., Mori, H. and Fukui, Y. (1984). Localization of actin and myosin for the study of amoeboid movement in *Dictyostelium* using improved immunofluorescence. *J. Cell Biol.* **99**, 894-899.